

NEW NONTHERMAL FILAMENTS AT THE GALACTIC CENTER: ARE THEY TRACING A GLOBALLY ORDERED MAGNETIC FIELD?

T. N. LAROSA

Department of Biological and Physical Sciences, Kennesaw State University, 1000 Chastain Road, Kennesaw, GA 30144; ted@avatar.kennesaw.edu

MICHAEL E. NORD

Department of Physics and Astronomy, University of New Mexico, Albuquerque, NM 87131; and Remote Sensing Division, Naval Research Laboratory, Washington, DC 20375-5351; Michael.Nord@nrl.navy.mil

AND

T. JOSEPH W. LAZIO AND NAMIR E. KASSIM

Remote Sensing Division, Naval Research Laboratory, Washington DC 20375-5351; joseph.lazio@nrl.navy.mil, namir.kassim@nrl.navy.mil

Received 2003 October 28; accepted 2004 January 29

ABSTRACT

New high-resolution, wide-field 90 cm VLA¹ observations of the Galactic center (GC) region by Nord and coworkers have revealed 20 nonthermal filament (NTF) candidates. We report 6 cm polarization observations of six of these. All of the candidates have the expected NTF morphology, and two show extended polarization, confirming their identification as NTFs. One of the new NTFs appears to be part of a system of NTFs located in the Sgr B region, 64 pc in projection north of Sgr A. These filaments cross the Galactic plane with an orientation similar to the filaments in the Galactic center radio arc. They extend the scale over which the NTF phenomena is known to occur to almost 300 pc along the Galactic plane. Another NTF was found in the Galactic plane south of the Sgr C filament but with an orientation of 45° to the Galactic plane. This is only the second of 12 confirmed NTFs that is not oriented perpendicular to the Galactic plane. An additional candidate in the Sgr C region was resolved into multiple filamentary structures. Polarization was detected only at the brightness peak of one of the filaments. Several of these filaments run parallel to the Galactic plane and can be considered additional evidence for nonpoloidal magnetic fields at the GC. Together the 90 and 6 cm observations indicate that the GC magnetic field may be more complex than a simple globally ordered dipolar field.

Subject headings: Galaxy: center — ISM: magnetic fields — radio continuum: ISM

1. INTRODUCTION

Understanding the origin, evolution, topology, and strength of the Galactic center (GC) magnetic field(s) is a necessary prerequisite for constructing a coherent picture of activity at the GC. The discovery of the Galactic center radio arc (GCRA; Yusef-Zadeh, Morris, & Chance 1984) demonstrated that magnetic structures with ordering on the scale of ~ 40 pc exist in the GC. The GCRA may also be part of an even larger scale structure known as the Omega lobe (Sofue & Handa 1984; Sofue 1985), which is a looplike structure extending several hundred parsecs from the GCRA and may connect with the Sgr C filament at its other footpoint. The ejection or expansion of a magnetic field from an accretion disk (Uchida, Sofue, & Shibata 1985; Heyvaerts, Norman, & Pudritz 1988) or a shocked Galactic wind (Chevalier 1992; Bland-Hawthorn & Cohen 2003) are possibilities for the origin of these structures. In addition, the discovery of isolated nonthermal filaments (NTFs) throughout the inner few hundred parsecs (e.g., Yusef-Zadeh & Bally 1989; Morris 1994; LaRosa et al. 2000) with orientations largely perpendicular to the Galactic plane have been interpreted as evidence for a space-filling poloidal field in the ionized medium (Morris & Serabyn 1996; Morris 1998). A pervasive poloidal field could result from the inflow of a primordial halo field toward the high concentration of mass

in the GC (Sofue & Fujimoto 1987; Chandran, Cowley, & Morris 2000; Chandran 2001) or from a nuclear starburst as stellar winds and supernovae inject stellar fields into the surrounding medium (Widrow 2002). Black hole accretion disks can also generate magnetic fields (e.g., Chakrabarti, Rosner, & Vainshtein 1994) that subsequently spread throughout the galaxy (Widrow 2002; Daly & Loeb 1990; Kronberg 2002 and references therein). Thus, both the ejection of dynamo-generated fields and the inflow and concentration of primordial fields could be acting independently to create the observed structures. Although these theoretical ideas are viable and reasonable, they have not been developed with sufficient rigor and detail to establish any definitive conclusions on the nature of magnetism at the GC.

Observationally, the NTFs are unique to the GC and are defined and identified by: (1) extreme length-to-width ratios (tens of parsecs long and only a few tenths of a parsec wide); (2) nonthermal spectral indices; and (3) high intrinsic polarization (for recent reviews, see Bicknell & Li 2001; LaRosa et al. 2003). Faraday rotation measurements indicate that the NTF magnetic fields are aligned longitudinally (e.g., Tsuboi et al. 1986; Yusef-Zadeh, Wardle, & Parastaran 1997; Lang, Morris, & Echevarria 1999b). Of the nine previously identified isolated NTFs—the most recent NTF discovery is described by Reich (2003)—eight of them, along with the bundled NTFs in the GCRA, are within 20° of the perpendicular to the Galactic plane. From the distribution and lengths of NTFs, it has been suggested that the magnetic field in the ionized medium is dominated by a poloidal field that extends many tens of parsecs

¹ The National Radio Astronomy Observatory (NRAO) is a facility of the National Science Foundation operated under a cooperative agreement by Associated Universities, Inc.

from the Galactic plane (e.g., Morris & Serabyn 1996; Morris 1998). (The lone NTF parallel to the plane, assuming a GC distance of 8 kpc [Reid 1993], is located southwest about 75 pc in projection from the Galactic plane and the farthest from Sgr A, approximately 225 pc in projection. It therefore could be in a region where the field lines are merging with the toroidal field in the disk [Lang et al. 1999a].)

Several estimates for the strength of NTF magnetic fields can be made. Estimates based on radio continuum measurements and assuming equipartition field strengths are of the order of a few tenths of a milligauss for several filaments (the Northern Thread, Lang et al. 1999b; the Sgr C filament, LaRosa et al. 2000; and the Snake filament, Gray et al. 1995). The absence of any bending or distortion of the NTFs against the strong ram pressure of the GC molecular clouds indicates a field strength of about 1 mG (Yusef-Zadeh & Morris 1987a, 1987b; see Chandran 2001 for further discussion of this point). Such a field strength is considerably stronger than the general interstellar magnetic field, which is typically no more than a few tens of microgauss (e.g., Crutcher 1999). The implied internal magnetic pressures of the NTFs are so large that unless they are confined by a comparable pressure, their lateral dimensions would expand well beyond the observed few tenths of a parsec on timescales short compared to their synchrotron lifetime. Confinement is not an issue if there is a ~ 1 mG field filling the entire region. In that case, the NTFs are the flux tubes that happen to be illuminated with high-energy electrons that are energized by some local interaction (Serabyn & Morris 1994). The energy density of such a space-filling field is quite high, of the order of 4×10^{-8} ergs cm^{-3} , and the total magnetic energy is $\sim 6 \times 10^{54} (R/75)^2 (L/300)$ ergs, where R and L are the radius and length (in pc) of the cylindrical region over which the NTF phenomenon is found.

However, alternatives to the pervasive field interpretation are also viable (e.g., Yusef-Zadeh 2003; Shore & LaRosa 1999). In the cometary model of Shore & LaRosa (1999), the NTFs are magnetized wakes generated by the interaction of molecular clouds with a GC wind. Considerable evidence for a Galactic wind is derived from X-ray observations of hot expanding gas (Koyama et al. 1996). The existence of a GC wind and related outflows is discussed in the context of recent high-resolution infrared observations by Bland-Hawthorn & Cohen (2003). In the cometary model, the wind is assumed to advect a weak ~ 10 μG magnetic field that is amplified by a factor of roughly 100 as the field is stretched by the flow and wraps around the obstacle, a molecular cloud, forming an elongated magnetotail (for quantitative details, see Gregori et al. 2000; Dahlburg et al. 2002). In this scenario, the total magnetic energy is reduced by several orders of magnitude, and presumably NTFs with every orientation could be observed since they are viewed in projection.

The above discussion indicates that additional observations are required to establish a consensus interpretation of the NTF phenomenon and its relationship to GC magnetism. This paper reports new total and polarized intensity observations of a number of NTF candidates that challenge the interpretation of a space-filling globally ordered poloidal field. In § 2 we describe the observations and analysis, and in § 3 we discuss the implications of our observations.

2. OBSERVATIONS AND RESULTS

Recently improved wide-field, high-sensitivity, high-resolution, VLA imaging of the GC at 90 cm (Nord et al. 2003)

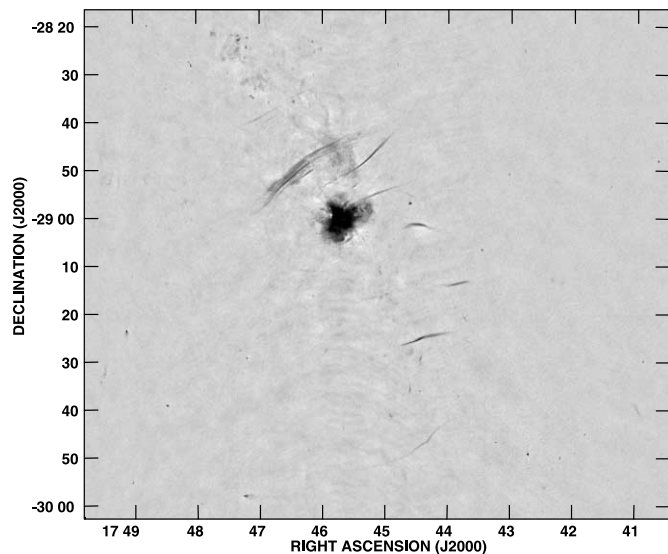


FIG. 1.—Inner 0.8×1.0 of the Galactic center region at 90 cm (Nord et al. 2003). The resolution is $7'' \times 12''$. This image was generated using a non-linear transfer function to simultaneously show the detail in the Sgr A region and the fainter NTFs

has revealed 20 new NTF candidates identified solely on the basis of their morphology. Figure 1 shows the inner 0.8×1.0 of the full 90 cm image produced by Nord et al. (2003). It was constructed from a combination of VLA A and B configuration observations, with a resulting resolution of $7'' \times 12''$. Although it is not sensitive to large-scale, low-surface brightness features, this image shows all previously known NTFs except for NTF 359.44+0.39, which was significantly resolved. The NTFs appear because their angular extent in one dimension is comparable to or smaller than the beam.

The previously known NTFs are mainly perpendicular to the Galactic plane. However, the orientations of the candidate NTFs are more diverse, with several nearly parallel to the plane. The candidates are also considerably shorter, with many less than 10 pc in length. The surface brightnesses of the candidates ($15\text{--}20$ mJy beam^{-1}) are roughly a factor of 4 or so less than the more prominent NTFs (Nord et al. 2003). In retrospect, a number of these candidates have been detected at higher frequencies. The candidate NTFs in the Sgr A region can be seen on the high-resolution 20 cm image of Lang et al. (1999b), who referred to shorter filamentary structures as “streaks.” In addition, several candidates near Sgr C were detected by Liszt & Spiker (1995) at 18 cm.

Although the morphologies of these NTF candidates are suggestive, spectra could not be constructed for all of them nor had any polarization observations been conducted. In order to confirm their status as NTFs, we conducted VLA observations of six of these sources at 6 cm in 2002 October. The observations were conducted with the VLA in the CnB configuration, providing a resolution of $4'' \times 3''$ (significantly higher than at 90 cm). Full polarization information was recorded.

The visibility data were calibrated and imaged using standard techniques within AIPS. Both total intensity (Stokes I) and linearly polarized intensity (Stokes Q and U) images were formed. The Galactic nonthermal background along the plane remains significant even at 6 cm and, despite integration times of several hours per source, it was not possible to achieve signal-to-noise ratios exceeding 5 in the total intensity images.

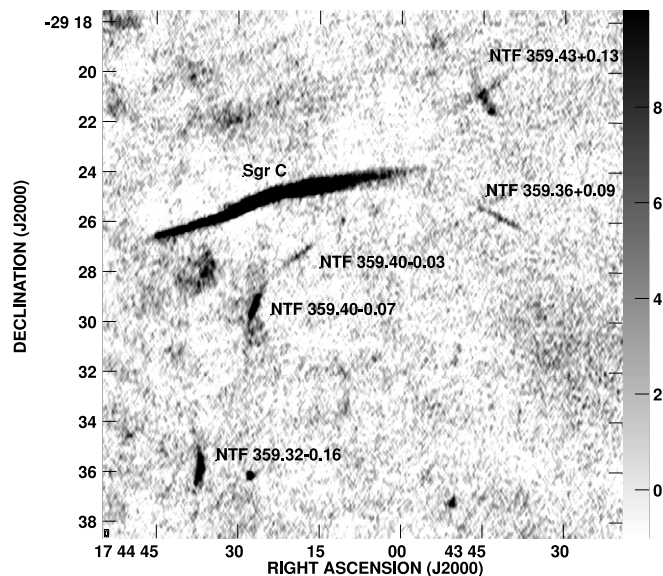


FIG. 2.—Sgr C region at 90 cm. Candidate NTFs are labeled with Galactic coordinates. The gray scale is linear between -1 and 10 mJy beam^{-1} .

The low signal-to-noise ratio also compromised our ability to detect polarization. In some cases, we were able to detect the total intensity emission from a source but no polarized emission. For the total linear polarized intensity [$L \equiv (Q^2 + U^2)^{1/2}$], a Rice-Nakagami distribution is obtained, and the upper limits we quote are relative to the rms noise level in the Q and U images, $\sigma_{Q,U}$. Nonetheless, these various limitations did not preclude our identifying a number of these candidates as NTFs.

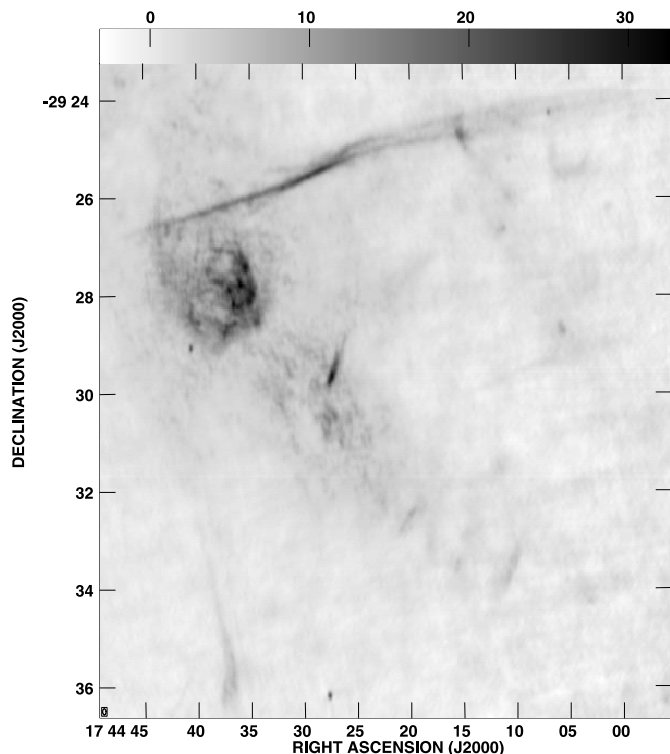


FIG. 3.—Sgr C region at 18 cm from Liszt & Spiker (1995) showing NTF 359.32–0.16 directly south of the H II region at R.A. = $17^{\text{h}}44^{\text{m}}37^{\text{s}}$ and decl. = $-29^{\circ}36'$. The resolution is $7''.5 \times 4''$.

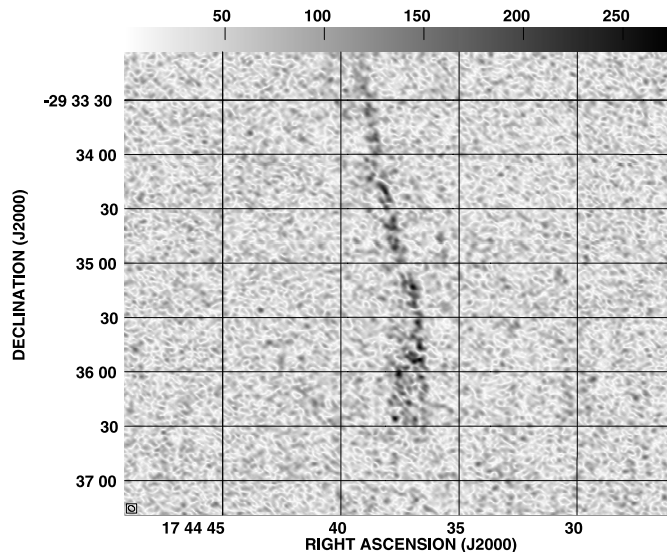


FIG. 4.—Polarized intensity image of NTF 359.32–0.16 at 6 cm. The resolution is $3''.75 \times 3''$, and the rms noise level is $25 \mu\text{Jy beam}^{-1}$. The gray scale is linear between 0 and $274 \mu\text{Jy beam}^{-1}$.

We concentrated on several candidates in the Sgr B and Sgr C regions, which we describe individually.

NTF 359.32–0.16.—Figure 2 shows a portion of the 90 cm image in the region of Sgr C. NTF 359.32–0.16 is located due south of the Sgr C H II region. This source is also detected at 18 cm (Liszt & Spiker 1995), as Figure 3 shows. The surface brightness at 18 cm is not uniform. The peak brightness ($\approx 7 \text{ mJy beam}^{-1}$) occurs at the southern terminus where the source is clearly wider, and the brightness decreases uniformly to 1 mJy beam^{-1} at the northern end. Intensity profiles perpendicular to the source's major axis show a clear double peak at the south end, suggesting that there may be two filaments in this system. The length of this source, assuming a GC distance of 8 kpc, is $\sim 8 \text{ pc}$. The 90 cm resolution is a factor of 3 poorer and does not show any structural details.

Figure 4 shows the 6 cm polarized image of NTF 359.32–0.16. Figure 5 shows the polarized intensity in gray scale overlaid with contours of total intensity. The polarization is patchy, similar to what is observed for other NTFs. The peak fractional polarization is 65%, and the average fractional polarization is $\sim 50\%$. This is consistent with the polarizations seen in other NTFs. The polarized image has a significantly better signal-to-noise ratio than the total intensity image, which is limited by the strong background emission from the Galactic plane. The object is also 8 pc long at 6 cm and $\leq 0.5 \text{ pc}$ wide. Given the similar beam sizes at 6 and 18 cm, we convolved the 6 cm image to the resolution of the 18 cm image and formed a series of intensity profiles at constant declination. These profiles were used to determine the peak brightness as a function of length along the structure and estimate the spectral index. The different spatial frequency (u - v) coverage in the 6 and 18 cm observations complicate the determination of an absolute spectral index. However, this analysis should reveal relative changes of spectral index with position. As Figure 6 illustrates, to within the uncertainties, the spectral index is constant, $\alpha_{6/18} \sim -1$ ($S \propto \nu^\alpha$), along the length of the filament. This constancy with position is consistent with other well-studied NTFs (Lang et al. 1999b; LaRosa et al. 2000). Spectral curvature appears to be another characteristic of the NTF phenomenon. Typical 20/90 cm and 6/20 cm spectral

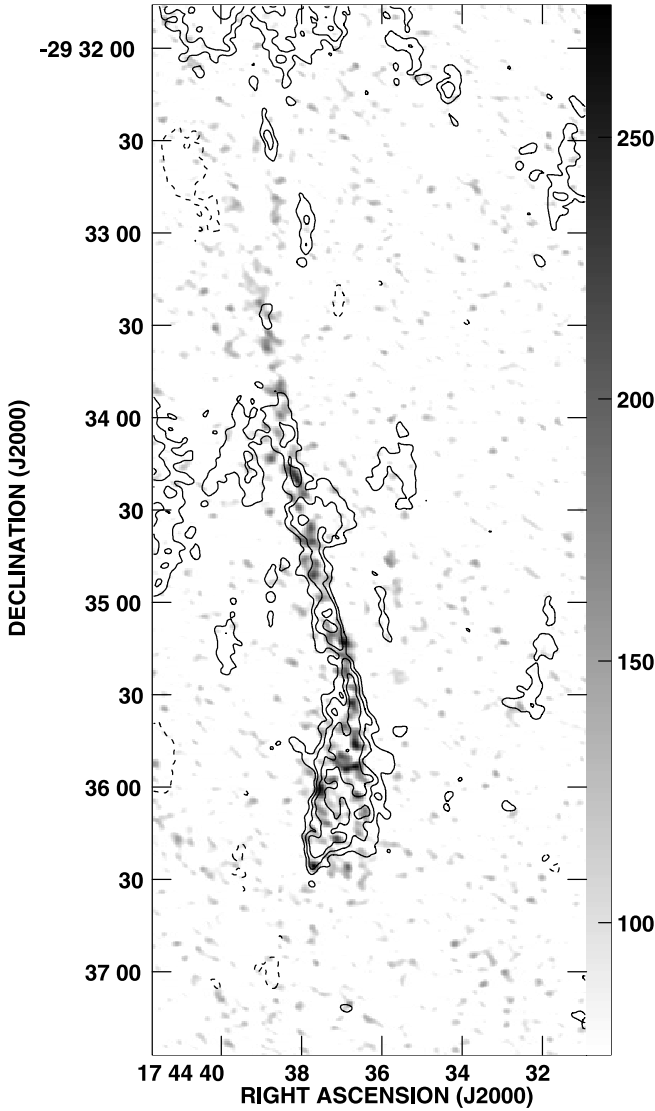


FIG. 5.—Total and polarized intensity images of NTF 359.32–0.16 at 6 cm. The beam is $3''.75 \times 3''$. The contours show the total intensity and are $0.2 \text{ mJy beam}^{-1}$ times $-2, 1.25, 2, 3, 5, 7.07$, and 10 , with the rms noise level in the total intensity image being $0.2 \text{ mJy beam}^{-1}$. The gray scale shows the polarized intensity and is linear between 75 and $275 \text{ } \mu\text{Jy beam}^{-1}$.

indices are between -0.4 and -0.6 , but above 5 GHz , the spectrum turns over (Lang et al. 1999b). Using the same method as described above, we estimated the $18/90 \text{ cm}$ spectral index near the location of the peak flux. We find that $\alpha_{18/90} \sim -0.1$. Thus, our $6/18 \text{ cm}$ index is steeper than typical, but our $18/90 \text{ cm}$ index is flatter. As we mentioned, determining an absolute spectral index is problematic, but we can confidently conclude that this source is nonthermal. Based on morphology, percentage polarization, and the nonthermal spectral index, we classify this source as an NTF.

NTF 359.43+0.13.—This candidate lies northwest of the Sgr C filament. At 90 cm it has a distinctive X-shape. Figure 7 shows that at 6 cm the X is resolved into a very bright, slightly elongated source with two, or perhaps three, longer filaments with significant curvature running roughly parallel to the Galactic plane and another filament perpendicular to these. Polarization of $\sim 10\%$ was detected near the location of the peak brightness. The signal-to-noise ratio along the filamentary structures is only 2 – 3 . Unfortunately, at this low signal-to-

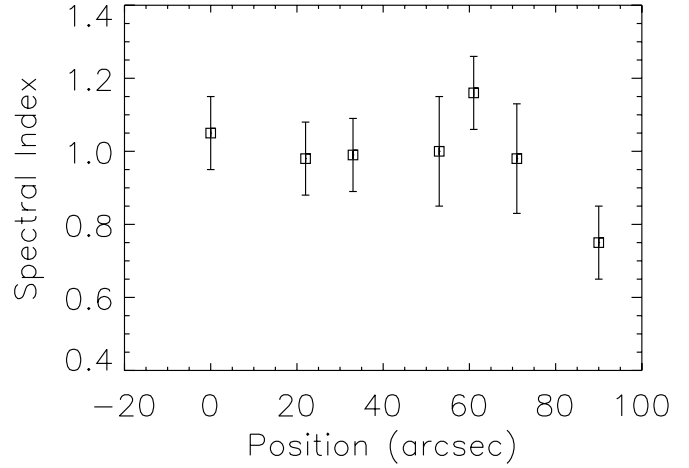


FIG. 6.— $6/18 \text{ cm}$ spectral index as a function of length along NTF 359.32–0.16. The error bars were determined from uncertainties in the base-lines of the individual crosscuts. The 0 position is located at R.A. = $17^{\text{h}}44^{\text{m}}37^{\text{s}}.5$, decl. = $-29^{\circ}36'01''$. The last position is located at R.A. = $17^{\text{h}}44^{\text{m}}37^{\text{s}}.5$, decl. = $-29^{\circ}34'31''$.

noise ratio, we would not have detected polarized emission even if these filaments were NTFs with high polarizations. Thus, we cannot state categorically that these sources are NTFs. However, given their morphology, it would be difficult to build a case for an alternative classification.

NTF 359.40–0.07.—This source is the brightest NTF candidate at 90 cm and lies 5 pc south in projection from the Sgr C filament. It was also detected at 18 cm (Liszt & Spiker 1995). We detect NTF 359.40–0.07 in total intensity at 6 cm , but we do not detect what appears to be a faint extension of this source in the 90 cm image (NTF 359.40–0.03). Using the 90 cm image to delineate the approximate extent of the source, we find the total linear polarization intensity distribution within this region to be noiselike, with no linear polarized emission above $4.5\sigma_{Q,U}$, where $\sigma_{Q,U} = 20 \text{ } \mu\text{Jy beam}^{-1}$. The lack of polarized emission (if the source is in fact polarized) may be a consequence of the strong background emission. To obtain a

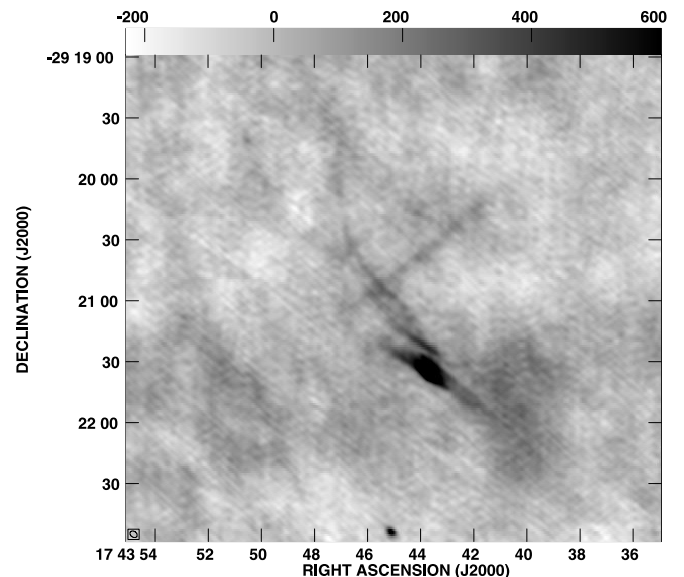


FIG. 7.—Total intensity image of NTF 359.43+0.13 at 6 cm . The resolution is $3''.9 \times 2''.8$, and the rms noise level is $66 \text{ } \mu\text{Jy beam}^{-1}$. The gray scale is linear between -228 and $600 \text{ } \mu\text{Jy beam}^{-1}$.

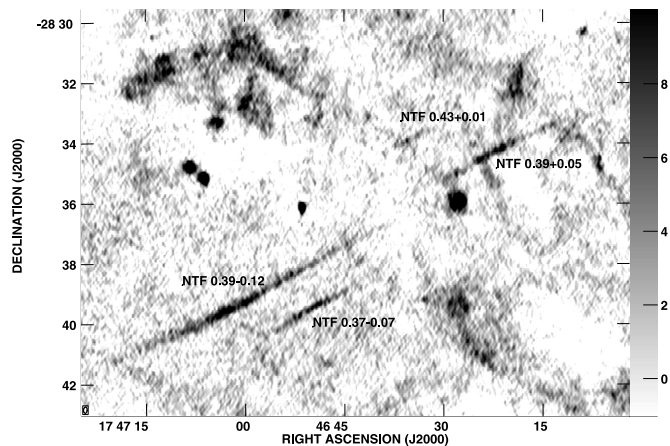


FIG. 8.—Sgr B region at 90 cm. Candidate NTFs are labeled with Galactic coordinates. The gray scale is linear between -1 and 10 mJy beam^{-1} .

rough estimate of the spectral index, we convolved the 6 cm map to the 18 cm map and made a few crosscuts near the location of the peak emission. We find that the 6/18 cm spectral index is $\alpha_{6/18} \sim -0.1$. Employing a similar procedure for the 18 and 90 cm maps, we estimate that the 18/90 cm spectral index is ~ 0.1 . There is considerable error in convolving the higher resolution maps to a larger beam in a confused region such as this, and we hesitate to draw any firm conclusions from these results. Further observations will be required to classify this source.

NTF 0.37–0.07, NTF 0.39+0.05, and NTF 0.39–0.12.—These three linear features are in the Sgr B region. Figure 8 shows the region at 90 cm (Nord et al. 2003), and Figure 9 shows the region at 6 cm. Due to the low signal-to-noise ratio only NTF 0.39–0.12 was detected in polarization (Fig. 10). The peak fractional polarization is 45%, while the average fractional polarization is $\sim 35\%$. It appears that NTF 0.39–0.12 and NTF 0.39+0.05 could be part of the same filament. Their clear linear morphology and similar orientation to the filaments in the GCRA strongly suggests that they are NTFs.

They are located about 64 pc in projection from Sgr A and are the first filaments found north of the GCRA. Although they are parallel to the GCRA filaments, they are located farther south of the Galactic plane. Thus, these objects extend the length scale (and therefore volume) over which the NTF phenomenon is

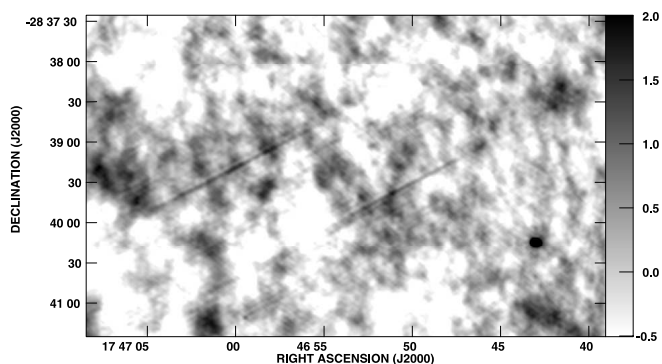


FIG. 9.—Newly discovered filaments in the Sgr B region at 6 cm. The straight filamentary nature of NTF 0.37–0.07 and NTF 0.39–0.12 is in this total intensity image. As shown in the next figure, NTF 0.39–0.12 is highly polarized. NTF 0.39+0.05 is too faint to be seen at this wavelength. The gray scale is linear between -0.5 and 2 mJy beam^{-1} . The beam is $3''.6 \times 2''.9$, and the rms noise level is $0.64 \text{ mJy beam}^{-1}$.

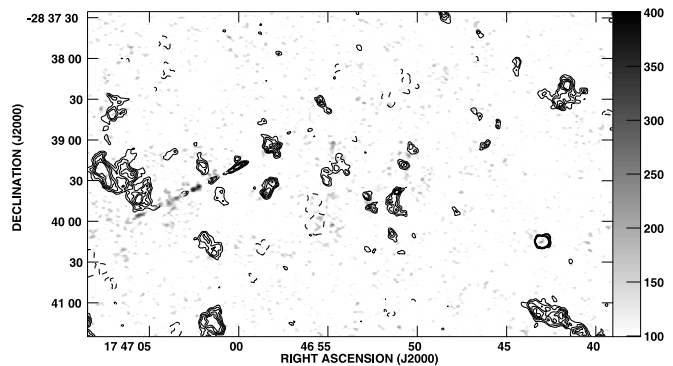


FIG. 10.—Total and linearly polarized intensity of NTF 0.39–0.12. The contours show the total intensity and are $0.64 \text{ mJy beam}^{-1}$ times $-2, 1.5, 1.75, 2, 2.25,$ and 2.5 . The gray scale shows the linearly polarized intensity and is linear between 100 and $400 \mu\text{Jy beam}^{-1}$.

known to occur to almost 300 pc along the Galactic plane. If the NTFs are a consequence of a global magnetic field, the field must be organized on at least this size scale.

3. DISCUSSION AND CONCLUSIONS

The 6 cm observations show that all the observed NTF candidates are filamentary in nature, with several of them showing polarization. Although only three of the six candidates exhibited the expected polarization, the low signal-to-noise ratio would have precluded detecting polarized emission from the remainder even if they were polarized at the level typical of NTFs. Generalizing these results, we conclude that many of the 90 cm NTF candidates probably are true NTFs. Consequently, there may be a large population of shorter, low-surface brightness NTFs.

Are these shorter, low-surface brightness NTFs the same class of phenomenon as the longer, brighter NTFs that are already known? Nord et al. (2003) shows that the typical surface brightness of the new filaments is approximately 20 mJy beam^{-1} at 90 cm; the surface brightness of the previously known filaments is 80 mJy beam^{-1} . The flux density S_ν as a function of frequency ν from a synchrotron source of volume V is $S_\nu \propto N_0 V B^{-\alpha+1} \nu^\alpha$, where N_0 is the number density of synchrotron-emitting electrons and B is the magnetic field within the volume. The widths of the new filaments are comparable to those of the previously known prominent NTFs, of the order of a few tenths of a parsec. Assuming that these are approximately cylindrical objects, then the volume element per unit length is the same for both the previously known and newly identified filaments. For a spectral index $\alpha \approx -1$, the luminosity of a synchrotron source scales with magnetic field as B^2 . Therefore, reproducing the observed range in surface brightnesses requires that the product $N_0 B^2$ vary by only a factor of 4. Either a factor of 4 variation in the synchrotron-emitting electron number density or a factor of 2 in the magnetic field strength is sufficient. Of course, if both N_0 and B vary, even smaller variations in each are required in order to obtain the required variation in $N_0 B^2$. We conclude that the same physical process could be responsible for the entire population, with small local variations in magnetic field strength and/or energetic particle density accounting for any differences.

A larger number of NTFs offers additional insights into the structure of any large-scale magnetic field. NTF 359.32–0.16 is oriented at an angle of 45° to the Galactic plane and is only the second NTF that is not oriented more-or-less perpendicularly

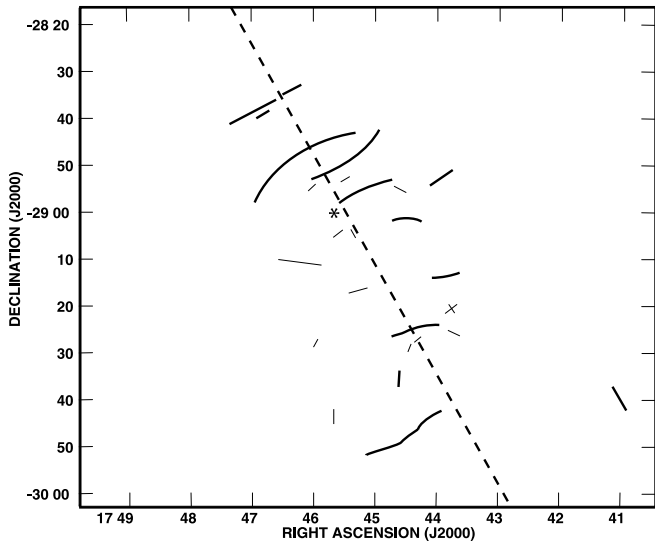


FIG. 11.—Schematic of the GC region based on the 90 cm wide-field image. Confirmed NTFs are shown in heavy dark lines. NTF candidates are shown in thin lines. The Galactic plane is the dashed line, and Sgr A is marked with an asterisk.

with respect to the Galactic plane. It is also considerably closer to Sgr A (87 pc in projection) than the other parallel NTF, NTF 358.85+0.47 (the Pelican). There is considerable evidence that the magnetic field in the neutral medium along the Galactic plane in the Sgr A and Sgr B regions is parallel to the plane (e.g., Novak et al. 2003),² suggesting that there is a large-scale toroidal field in the neutral medium. Given its 45° orientation, it seems unlikely that this NTF is related to a toroidal field. Furthermore, SCUBA images (Pierce-Price et al. 2000) of the GC indicate that the thermal emission from the Sgr C environment is much less than in the Sgr A or Sgr B regions. Thus, the region near Sgr C, including NTF 359.32–0.16, may not be dominated by the neutral medium.

Figure 11 is a schematic of the GC region based on the wide-field image of Nord et al. (2003). The confirmed NTFs (including those from this work) are shown in the heavy dark lines, while the NTF candidates are denoted by the thin lines. Confirmation of additional candidates would definitively rule out a global dipole field model. However, the present data are already difficult to reconcile with global ordering. Figure 11 shows that there are several cases where two NTFs, which are close together in projection, have very different orientations. In order to preserve $\nabla \cdot \mathbf{B} = 0$ in a region of space, distinct

field lines must be more or less parallel on scales smaller than any gradient scale. The northern end of NTF 359.32–0.16 is 15 pc in projection from the Sgr C filament and has an orientation $\sim 45^\circ$ to it. The Sgr C filament is about 30 pc long and, although it has a nonuniform brightness, it exhibits a constant spectral index with length, suggesting that it is tracing a uniform magnetic field. For a dipole magnetic field, $B/\nabla B = r/3$, where r is the radial distance from the dipole. For a dipolar field centered on Sgr A at the location of NTF 359.32–0.16 (87 pc in projection), the gradient scale length is almost 30 pc, consistent with the Sgr C NTF. However, if NTF 359.32–0.16 is at the same distance with a 45° difference in orientation, it could not be tracing the same divergence-free field. Another example is the Northern Thread NTF 0.08+0.15 and the NTF candidate G359.90+0.19. These two are separated by only about 5 pc in projection and both are about 30 pc in projection from Sgr A, yet their orientations differ by 25°.

These differences in orientation cannot be explained as being due to differences in their relative distances. While little is known about their relative separations, as noted earlier, the NTF phenomenon occurs over a linear distance of roughly 300 pc along the Galactic plane ($-1^\circ \lesssim l \lesssim 0.4^\circ$). It is reasonable to assume that the NTFs are also distributed over a comparable distance along the line of sight. If this is the case, large apparent changes in orientation could be obtained in a dipolar field by filaments well above the Galactic plane and located at different distances along the line of sight (e.g., the Northern Thread NTF 0.08+0.15 and the NTF candidate G359.90+0.19). Even so, if the GC magnetic field is poloidal and dominated by a dipolar component, all filaments crossing the Galactic plane should be nearly perpendicular to the Galactic plane, regardless of their distance along the line of sight. The different orientations of the Sgr C filament and NTF 359.32–0.16 demonstrate that the GC magnetic field cannot be dominated by a largely dipolar poloidal component.

The new 90 cm survey coupled with the 6 cm observations described here indicate that the population of GC NTFs is significantly larger than previously thought. These new NTFs cannot be interpreted as components of a globally ordered poloidal magnetic field and suggest a more complicated field structure. Further, high-sensitivity observations, especially with new instrumentation such as the expanded VLA and LOFAR (see Kassim et al. 2003; White, Kassim, & Erickson 2003) will be required to discover and characterize the entire population of GC NTFs.

We thank Harvey Liszt for sharing his 18 cm Sgr C data and Steve Shore for many stimulating discussions concerning Galactic center physics. We also thank the referee M. Sakano for a thoughtful reading of the manuscript that significantly improved the paper. Basic research in radio astronomy at the NRL is supported by the Office of Naval Research.

REFERENCES

- Bicknell, G., & Li, J. 2001, *Publ. Astron. Soc. Australia*, 18, 431
 Bland-Hawthorn, J., & Cohen, M. 2003, *ApJ*, 582, 246
 Chakrabarti, S. K., Rosner, R., & Vainshtein, S. I. 1994, *Nature*, 368, 434
 Chandran, B. D. G. 2001, *ApJ*, 562, 737
 Chandran, B. D. G., Cowley, S. C., & Morris, M. 2000, *ApJ*, 528, 723
 Chevalier, R. A. 1992, *ApJ*, 397, L39
 Chuss, D. T., Novak, G., Hildebrand, H., Dowell, C. D., Vaillancourt, J. E., Davidson, J. A., & Dotson, J. L. 2004, *ApJ*, in press
 Crutcher, R. M. 1999, *ApJ*, 520, 706
 Dahlburg, R. B., Einaudi, G., LaRosa, T. N., & Shore, S. N. 2002, *ApJ*, 568, 220
 Daly, R. A., & Loeb, A. 1990, *ApJ*, 364, 451
 Gray, A. D., Nicholls, J., Ekers, R. D., & Cram, L. E. 1995, *ApJ*, 448, 164
 Gregori, G., Miniati, M., Ryu, D., & Jones, T. W. 2000, *ApJ*, 543, 775
 Heyvaerts, J., Norman, C., & Pudritz, R. E. 1988, *ApJ*, 330, 718
 Kassim, N. E., Lazio, T. J. W., Nord, M., Hyman, S. D., Brogan, C. L., LaRosa, T. N., & Duric, N. 2003, in *The Central 300 Parsecs of the Milky Way* (*Astron. Nachr. Suppl.*, 324 [1]), 65

- Koyama, K., Maeda, Y., Sonobe, T., Takeshima, T., Tanaka, Y., & Yamauchi, S. 1996, *PASJ*, 48, 249
- Kronberg, P. P. 2002, *Phys. Today*, 55, 40
- Lang, C. C., Anantharamaiah, K. R., Kassim, N. E., Lazio, T. J. W., & Goss, W. M. 1999a, *ApJ*, 521, L41
- Lang, C. C., Morris, M., & Echevarria, L. 1999b, *ApJ*, 526, 727
- LaRosa, T. N., Kassim, N. E., Lazio, T. J. W., & Hyman, S. D. 2000, *AJ*, 119, 207
- LaRosa, T. N., Nord, M. E., Lazio, T. J. W., & Kassim, N. E. 2003, in *The Central 300 Parsecs of the Milky Way* (*Astron. Nachr. Suppl.*, 324 [1]), 181
- Liszt, H. S., & Spiker, R. 1995, *ApJS*, 98, 259
- Morris, M. 1994, in *The Nuclei of Normal Galaxies*, ed. R. Genzel & A. I. Harris (NATO ASI Ser. C, 445; Dordrecht: Kluwer), 185
- . 1998, in *IAU Symp. 184, The Central Regions of the Galaxy and Galaxies*, ed. Y. Sofue (Dordrecht: Kluwer), 331
- Morris, M., & Serabyn, E. 1996, *ARA&A*, 34, 645
- Nord, M. E., Brogan, C. L., Hyman, S. D., Lazio, T. J. W., Kassim, N. E., LaRosa, T. N., Anantharamaiah, K., & Duric, N. 2003, in *The Central 300 Parsecs of the Milky Way* (*Astron. Nachr. Suppl.*, 324 [1]), 9
- Novak, G., et al. 2003, *ApJ*, 583, L83
- Pierce-Price, D., et al. 2000, *ApJ*, 545, L121
- Reich, W. 2003, *A&A*, 401, 1023
- Reid, M. J. 1993, *ARA&A*, 31, 345
- Serabyn, E., & Morris, M. 1994, *ApJ*, 424, L91
- Shore, S. N., & LaRosa, T. N. 1999, *ApJ*, 521, 587
- Sofue, Y. 1985, *PASJ*, 37, 697
- Sofue, Y., & Fujimoto, M. 1987, *PASJ*, 39, 843
- Sofue, Y., & Handa, T. 1984, *Nature*, 310, 568
- Tsuboi, M., Inoue, M., Handa, T., Tabara, H., Kato, T., Sofue, Y., & Kaifu, N. 1986, *AJ*, 92, 818
- Uchida, Y., Sofue, Y., & Shibata, K. 1985, *Nature*, 317, 699
- White, S., Kassim, N. E., & Erickson, W. C. 2003, *Proc. SPIE*, 4853, 111
- Widrow, L. M. 2002, *Rev. Mod. Phys.*, 74, 775
- Yusef-Zadeh, F. 2003, *ApJ*, 598, 325
- Yusef-Zadeh, F., & Bally, J. 1989, in *IAU Symp. 136, The Center of the Galaxy*, ed. M. Morris (Dordrecht: Kluwer), 197
- Yusef-Zadeh, F., & Morris, M. 1987a, *ApJ*, 322, 721
- . 1987b, *AJ*, 94, 1178
- Yusef-Zadeh, F., Morris, M., & Chance, D. 1984, *Nature*, 310, 557
- Yusef-Zadeh, F., Wardle, M., & Parastaran, P. 1997, *ApJ*, 475, L119